OPEN

PRS GLOBAL OPEN

ORIGINAL ARTICLE
Research

Experimental Study of Warburg Effect in Keloid Nodules: Implication for Downregulation of miR-133b

Yuumi Lee, MD*
Yuko Ito, MD, PhD†
Kohei Taniguchi, MD, PhD‡
Takashi Nuri, MD, PhD*
SangWoong Lee, MD, PhD†
Koichi Ueda, MD, PhD*

Background: A keloid is composed of several nodules, which are divided into two zones: the central zone (CZ; a hypoxic region) and the marginal zone (MZ; a normoxic region). Keloid nodules play a key role in energy metabolic activity for continuous growth by increasing in number and total area. In this study, we aimed to investigate the roles of the zones in the execution of the Warburg effect and identify which microRNAs regulate this phenomenon in keloid tissue.
Methods: Eleven keloids from patients were used. Using immunohistochemical analysis, 179 nodules were randomly chosen from these keloids to identify glycolytic enzymes, autophagic markers, pyruvate kinase M (PKM) 1/2, and polypyrimidine tract binding protein 1 (PTBP1). Western blot and qRT-PCR tests were also performed for PKM, PTBP1, and microRNAs (miR-133b and miR-200b, c).
Results: Immunohistochemical analysis showed that the expression of the autophagic (LC3, p62) and glycolytic (GLUT1, HK2) were significantly higher in the CZ than in the MZ. PKM2 expression was significantly higher than PKM1 expression in keloid nodules. Furthermore, PKM2 expression was higher in the CZ than in the MZ. However, PKM1 and PTBP1 expression levels were higher in the MZ than in the CZ. The qRT-PCR analysis showed that miR-133b-3p was moderately downregulated in the keloids compared with its expression in the normal skin tissue.
Conclusions: The Warburg effect occurred individually in nodules. The MZ presented PKM2-positive fibroblasts produced by activated PTBP1. In the CZ, PKM2-positive fibroblasts produced lactate. MiR-133b-3p was predicted to control the Warburg effect in keloids. *(Plast Reconstr Surg Glob Open 2023; 11:e5202; doi: 10.1097/GOX.0000000000005202; Published online 16 August 2023.)*

INTRODUCTION

Keloids are cutaneous fibro-proliferative disorders characterized by excessive scarring and collagen formation. We have previously reported that keloid tissues express high ATP levels and maintain their characteristic structure, even after 10 years,[1] whereas nodules express metabolic activity for continuous expansion of keloid tissues.[2,3] Keloid nodules are composed of two zones. The central zone (CZ) is a hypoxic zone due to the presence of aberrant flattened blood vessels and the production and export of lactate. This might be due to a higher expression of glycolytic, autophagic, and lactate secretion protein markers, as well as an increased L-lactate production and increased levels of monocarboxylate transporter 4 (MCT4) expression in fibroblasts. The marginal zone (MZ), which surrounds the CZ nests, is a normoxic and oxidative phosphorylation (OXPHOS) zone formed by a circular layer of collagen bundles rich in blood vessels.[2,3] Furthermore, the MZ endothelial cells and fibroblasts express proliferative nuclear antigens and hypoxia-inducible factor 2-α (HIF2-α). Fibroblasts in the MZ also express monocarboxylate transporter 1 (MCT1). It is characteristic of the CZ and MZ to sustain energy and proliferation; however, further research is required to determine the

*From the *Department of Plastic and Reconstructive Surgery, Osaka Medical and Pharmaceutical University, Osaka, Japan; †Department of General and Gastroenterological Surgery, Osaka Medical and Pharmaceutical University, Osaka, Japan; and ‡Center for Medical Research & Development, Division of Translational Research, Osaka Medical and Pharmaceutical University, Osaka, Japan.*

Received for publication April 17, 2023; accepted July 6, 2023.

Presented at The 2nd World Congress of Global Scar Society with Scar Academy, 2021, Yokohama, Japan, and at the 30th Research Council Meeting of Japan Society of Plastic and Reconstructive Surgery, 2021, Okayama, Japan.

DOI: 10.1097/GOX.0000000000005202

Disclosure statements are at the end of this article, following the correspondence information.

Related Digital Media are available in the full-text version of the article on www.PRSGlobalOpen.com.

factors executing glycolysis, including the pyruvate kinase family proteins and microRNAs (miRNAs), and the role of each zone in energy acquisition.

The Warburg effect refers to the observation that cancer cells produce energy (ATP) by glycolysis in both anaerobic and aerobic conditions.[4] It yields not only ATP from glucose but also nucleic acids, proteins, lipids, and sugars necessary for proliferation, which are active as byproducts in the glucose metabolism process.[5] The reverse Warburg effect was proposed by Pavlides et al[6] as a new model to understand stromal-epithelial metabolic coupling in cancer. To explain the high ATP levels found in keloid tissues, Vincent et al[7] reported that cultured keloid fibroblasts show bioenergetics similar to that of cancer cells as they generate ATP mainly from glycolysis, even under aerobic conditions. Another study demonstrated that, at the protein and mRNA levels, keloid fibroblasts show a higher expression of glycolytic enzymes than do normal skin fibroblasts.[8] Glycolysis is induced by glycolytic enzymes, pyruvate kinase M (PKM) 1/2, or pyruvate kinase L/R (PKLR). PKM 1/2 catalyzes the final step in glycolysis, and polypyrimidine tract binding protein 1 (PTBP1) is essential to produce PKM2 for the Warburg effect.[9]

MiRNAs are noncoding functional small RNAs that modify gene expression at the translational level and have become a new basis for therapeutic strategies for cancer and other diseases.[10,11] Research on nucleic acid therapeutics using miRNAs against cancer are no more at a level of infancy; such therapeutics are undergoing phase I and II testing in humans.[12–15] Some organ-specific miRNAs regulate PKM isoform expression by directly targeting *PTBP1*, which is the splicer responsible for PKM2-dominant expression.[16] The miRNAs targeting *PTBP1* are extensively studied because of their role in regulating cancer-specific energy metabolism (ie, the Warburg effect).[17]

The miRNA expression profiles of keloids were examined by miRNA microarray analysis and qRT-PCR analyses to elucidate the underlying pathogenesis of keloids.[18] These previous studies show that keloid fibroblasts have a great capacity for aerobic and anaerobic glycolysis. However, the pathogenesis of the resulting glycolysis and by which the Warburg and reverse Warburg effects are sustained in keloid tissues remains unclear. A deeper understanding of the Warburg effect and its development may result in the discovery of a new therapy method. Hence, here we investigated the final promoter for glycolysis, the miRNAs involved in its regulation, and the roles of the two keloid zones involved in the Warburg effect.

Takeaways

Question: The aim of this study was to investigate the execution of the Warburg effect (anaerobic and aerobic glycolysis), and which miRNA controls the Warburg effect in nodules which are composed of central (CZ) and marginal (MZ) zones.

Findings: The keloid produced energy by the Warburg effect in individual nodules. Pyruvate kinase M1/2 and polypyrimidine tract binding protein 1 were essential to execute the Warburg effect. Downregulation of miR-133b-3p was demonstrated in keloids.

Meaning: MiR-133b-3p is predicted to control the Warburg effect in keloid tissue, and could be an excellent noninvasive tool for keloid diagnosis, prognostication, and treatment.

MATERIALS AND METHODS

Patients and Samples

We resected 11 keloid (duration times: 0.8, 2.2, 3, 4, 5, 10, 13, 20 years) and six normal skin tissue samples at Osaka Medical and Pharmaceutical University Hospital from November 2018 to October 2019 (Table 1). Normal skin samples were obtained from the trunks of healthy donors during plastic surgery procedures. The study was approved by the institutional review board of Osaka Medical Pharmaceutical University (acceptance no.: 1892-3), and written informed consent was obtained from all patients.

Table 1. Patient and Sample Characteristics and Treatment Details

Case	Age	Sample	Etiology	Region	Disease Duration	History of Intralesional Corticosteroid Injections	JSW Scar Scale
1	30	K1	Cesarean section	Abdomen	2 y 2 mo	5 times	NA
2	66	K2	Cesarean section	Abdomen (epigastric region)	4 y 8 mo	–	NA
		K3		Abdomen (hypogastoric region)		–	
3	38	K4	Unknown	Forearm	10 y	–	20/25
4	40	K5	Endoscopic surgery	Abdomen	3 y	–	8/25
5	27	K6	injection	Shoulder	20 y	–	19/25
		K7		Upper arm		–	
		K8	Injury	Elbow	13 y	–	NA
7	18	K9	Acne scar	Chest	4 y	–	19/25
		K10		Shoulder		–	
8	35	K11	Thyroidectomy	Neck	8 mo	–	13/25

JSW, Japan Scar Workshop.

Western Blotting

Keloid and skin samples were homogenized and lysed with cold RIPA buffer (Thermo Fisher Scientific Inc., Waltham, Mass.) and a 1% Protease Inhibitor Cocktail (Sigma-Aldrich, St. Louis, Mo.). The SDS-PAGE procedure was performed as described in our previous study.[16] The primary antibodies used for western blotting were anti-PKM1 (D30G6, 1:1000, Signaling Technology Inc., Danvers, Mass.), anti-PKM2 (D78A4, 1:1000, Signaling Technology), and anti-PTBP1 (ab30317, 1:1000, Abcam, Cambridge, United Kingdom). An anti-β-actin antibody (7076S, 1:1000, Signaling Technology) was used as a standard for quantitative protein analysis.

Histopathology

The specimens were fixed in 10% formalin, embedded in paraffin, and cut into 5-μm sections for hematoxylin and eosin (H&E) staining and immunohistochemical analysis.

Transmission Electron Microscopy

To identify the ultrastructural differences between fibroblasts in the CZ and MZ, the specimens were treated as described in our previous study[19] and observed by Transmission Electron Microscopy (Hitachi-7800, Tokyo, Japan).

Immunohistochemical Analysis

Immunohistochemical (IHC) analyses were performed according to our previous study.[2] The sections were then incubated with primary antibodies anti-LC3 (#27751, 1:100, Signaling Technology), anti-p62 (18420-1-Ap, 1:100, Proteintech, Rosemont, Ill.), anti- hexokinase 2 (HK2;22029-1-Ap, 1:100, Proteintech), antiglucose transporter 1 (GLUT1;ab115730, 1:100, Abcam), and the same antibodies used in western blotting [ie, anti-PKM1 (1:25), PKM2 (1:200), and PTBP1 (1:100)]. The labeled sections were observed and captured using a fluorescent microscope (BZ-X800, Keyence, Osaka, Japan).

Measurement Procedure

The nodules in the keloids were identified on H&E staining as described in our previous study.[2] In total, 179 nodules were randomly chosen from the 11 keloid samples with previously identified/evaluated CZs and MZs. Using Photoshop (Adobe Inc., San Jose, Calif.) and ImageJ (National Institutes of Health, Bethesda, Md.), the area of a nodule, MZ, and CZ were measured and analyzed. [**See figure, Supplemental Digital Content 1**, which shows the measurement procedure. The evaluated zone (red) and immune-positive areas (red dots) were captured using Photoshop and the measured area by pixel using ImageJ. **http://links.lww.com/PRSGO/C734**.]

Single and Double-labeling Immunofluorescence

To demonstrate that fibroblasts express Warburg effect-related markers, single- and double-labeling fluorescent analyses of the keloid samples were performed as described in our previous study.[2] The primary antibodies were the same as those used in IHC analysis, including antivimentin (V4630, 1:40, Sigma-Aldrich). The secondary antibodies used were Alexa Fluor 594 chicken antirabbit or Alexa Fluor 488 donkey antigoat antibodies (1:250, Life Technologies, Inc., Rockville, Mo.). The labeled sections were observed with a fluorescent microscope (BZ-X800, Keyence).

miRNA Extraction and Quantitative Real-time PCR (qRT-PCR)

We explored the mechanism of PTBP1 activation with a focus on miRNA expression. Extensive analysis using the Target Scan Human version 7.2 website (**https://www.targetscan.org/vert_72/**) indicated that miR-133b, miR-200b, and miR-200c were the *PTBP1*-targeting miRNAs. Total RNA was isolated from keloids and skin tissues using a NucleoSpin miRNA isolation kit (TaKaRa Bio Inc., Shiga, Japan). To determine the expression levels of miR-133b-3p, miR-200b-3p, and miR-200c-3p, we conducted qRT-PCR tests as described in our previous study.[20] Each ΔΔCt value was determined using the Thermal Cycler Dice Real-Time System II model TP870 (Takara Bio Inc.). RNU6B was used as an internal control. The qRT-PCR tests were performed with the primers listed in Table 2 using THUNDERBIRD SYBR qPCR Mix (TOYOBO, Osaka, Japan).

Statistical Analysis

Data analysis was performed using StatMateIII (ATMS, Chiba, Japan). A Mann–Whitney test was used to compare continuous variables between groups. Results were expressed as mean ± SD (SD), where relevant. According to the results, *P* values less than 0.01 were considered statistically significant.

RESULTS

Detection and Histological Characterization of Nodules

Following H&E staining of the keloid tissues (Fig. 1A) at the dermis layer (marked by asterisks), we identified nodules that showed thick hyaline collagen fibers with

Table 2. Validations of miRNAs Used in this Study

miRNA Gene Name (ID)	miR133b (442890)	miR200b (406984)	miR200c (406985)
Target gene name (ID)	PTBP1 (5725)	PTBP1 (5725)	PTBP1 (5725)
Species name (ID)	Homo sapiens (9606)	Homo sapiens (9606)	Homo sapiens (9606)
Genomic location of Nucleotide sequence	5'GACCAA	5'CAGUAUU	5'CAGUAUU
Primer sequence	UUUGGUCCCCUUCAACCAGCUA	UAAUACUGCCUGGUAAUGAUGA	UAAUACUGCCGGGUAAUGAUGGA

serious eosinophilia. The nodules consisted of the CZ and MZ regions (Fig. 1B). Concordant with the results from our previous study, many more serial vessels were found with a wider lumen in the MZ than in the CZ region (Fig. 1B).

The TEM analysis revealed ultrastructural differences between fibroblasts in the CZ and MZ. The CZ fibroblasts had many autophagic vacuoles in their cytoplasm (Supplemental Digital Content 2A, 2B) and a few apoptotic cells (Supplemental Digital Content 2C). In contrast, MZ fibroblasts had well-reserved mitochondria and well-developed rough endoplasmic reticulum (rER), which resulted in the accumulation of proteins that were generated in their ribosomes [**See figure, Supplemental Digital Content 2,** which shows ultrastructural features of fibroblasts in the CZ and MZ. A–C, Fibroblast in the CZ. CZ fibroblasts showed autophagic or apoptotic features. Thin arrows: fibroblast; red marked arrows: autophagic vacuoles; yellow marked arrows: apoptotic nucleus showing condensed chromatin; white arrow: autolysosome. D, Fibroblasts in the MZ. MZ fibroblast showed prominent active features in protein synthesis. Blue marked arrow: dilated endoplasmic reticulum. In A–C, Cf: collagen fiber, m: mitochondrion, N: nucleus. **http://links.lww.com/PRSGO/C735**.]

Keloid Tissue Demonstrated Glycolysis and Autophagic Markers

Enhancement of Glycolysis and Autophagy Occurred in the CZ

Fibroblasts in nodules that expressed glycolytic (HK2, GLUT1) and autophagic markers (LC3, p62) showed the same distribution patterns in different zones, with a strong expression localized in the CZ (Supplemental Digital Content 3 in top row). The value of the positive area of both glycolytic and autophagic markers was significantly higher in the CZ than in the MZ region

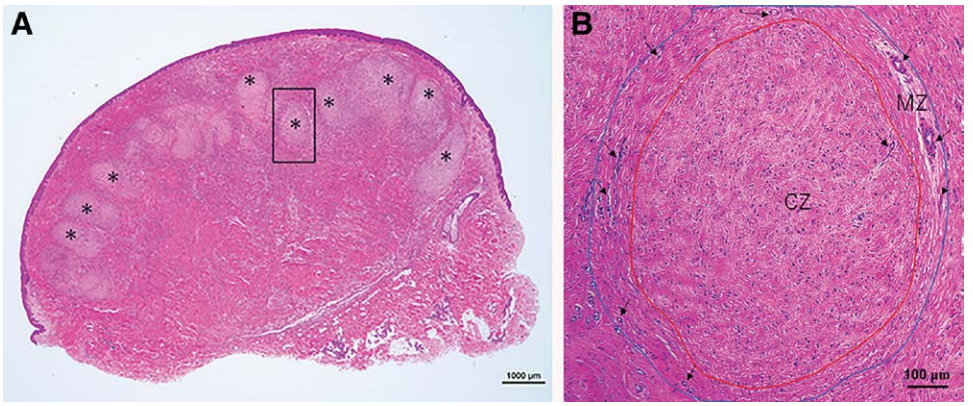

Fig. 1. Pathological features of a keloid and identification of zones. A, Hematoxylin and eosin staining of keloids (K5) as mentioned in Table 1. Many nodules (*) were located in the dermis and/or subcutaneous tissue in a keloid. B, A nodule in the boxed area in A was enlarged. Many blood vessels (arrows) were localized in the MZ, whereas fewer vessels (arrow) were observed in the CZ.

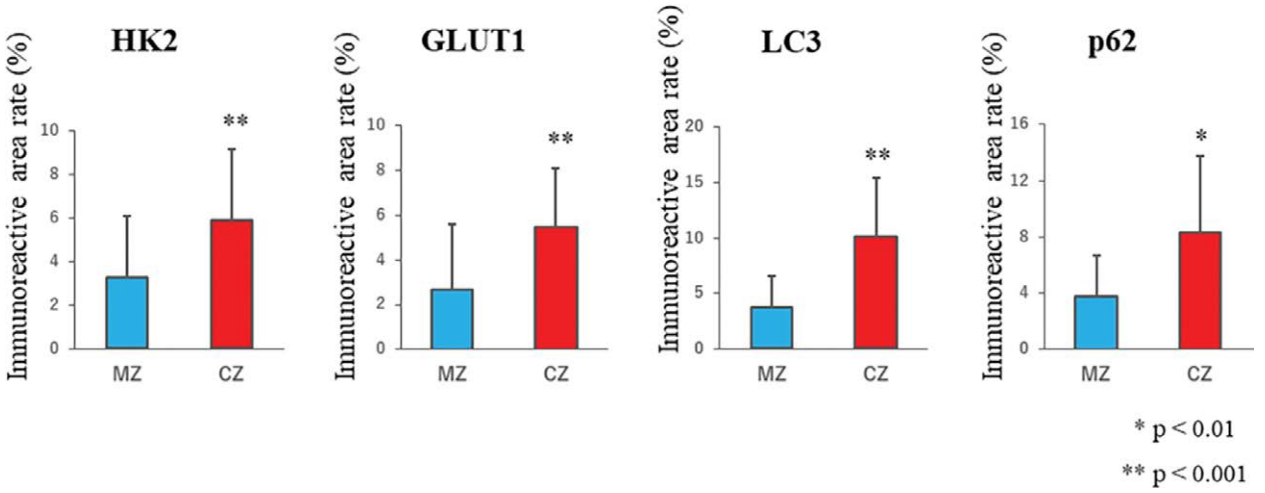

Fig. 2. Enhanced expression of glycolytic and autophagic markers in nodules. Immunohistochemical analysis of the glycolytic (HK2, GLUT1) and autophagic (LC3, p62) markers in nodules. ImageJ analysis showed glycolytic markers and autophagic markers were significantly increased in the CZ (*P < 0.01, **P < 0.001). Numbers represent the percentage of the immunoreactive area per zone.

($P < 0.01$) (Fig. 2). [**See figure, Supplemental Digital Content 3,** which shows immunohistochemical analysis. Top row: glycolytic (HK2, GLUT1) and autophagic (LC3, p62) markers in nodules; bottom row: Warburg effect markers (PKM1, PKM2, and PTBP1) in nodules. A dark brown area showed immunopositive fibroblasts. The dark blue lines indicate the area of a nodule, and the red lines show the border between the MZ and CZ. **http://links.lww.com/PRSGO/C736**.]

The Execution of the Warburg Effect in Skin and Keloid Tissues

Warburg Effect Marker Was Expressed in Keloids

After western blot analyses of PKM1, PKM2, and PTBP1 in skin and keloid tissues (Fig. 3A), the β-actin loading control was found highly expressed in keloids and had to be corrected for comparisons (Fig. 3B). We found that the levels of PKM1 and PKM2 in keloids were similar to those in the skin, and the expression of PKM2 was higher in keloids than in the skin (Fig. 3B), whereas PTBP1 expression was significantly higher in the skin than in keloids ($P < 0.01$) (Fig. 3B).

Keloid Nodules and the CZ Showed Robust Expression of PKM2, and the MZ Showed Strong Expression of PKM1 and PTBP1

Fibroblasts in nodules expressing PKM2 showed a localized distribution in the CZ, whereas fibroblasts expressing PKM1 and PTBP1 showed a diffuse distribution in nodules (Supplemental Digital Content 3 in bottom row). ImageJ results from IHC analyses showed that, in the nodule, the total PKM2-positive area was significantly higher than that of PKM1 (**$P < 0.001$). In the MZ, there was an enhanced expression of PKM1 (10.25 ± 12.45) and PTBP1 (3.22 ± 2.54), and in the CZ, there was a modestly higher expression of PKM2 (12.85 ± 7.085) than that of the proteins in the other surrounding zones (Fig. 3C).

Fibroblasts in Nodules Expressing Warburg Effect Markers

After double immunofluorescent staining for vimentin (fibroblast marker) and Warburg effect markers (PM1, PKM2, PTBP1), we found localized fibroblasts expressing Warburg effect markers in the CZ and MZ. [**See figure, Supplemental Digital Content 4,** which shows the double-labeling immunofluorescent micrographs. The Warburg effect markers (red) with vimentin (a fibroblast marker, green) were indicated in the CZ and the MZ. 4'6-diamidino-2-phenylindole (DAPI, blue) was used to stain the nucleus. Left column: PKM1; middle column: PKM2; left column: PTBP1. The positive area of the Warburg effect markers is overlapped with vimentin signals. **http://links.lww.com/PRSGO/C737**.]

Downregulation of *PTBP1*-targeting miRNA in Keloids

The qRT-PCR tests with primers for miR-133b-3p, 200b-3p, and 200c-3p showed a moderately lower expression of miR-133b-3p in keloids than in the skin (**$P < 0.001$) (Fig. 4).

DISCUSSION

Using clinical keloid specimens and IHC analysis, we confirmed that the Warburg effect occurs in each nodule of keloids. In addition, we found moderate lower expression of miR-133b-3p in keloid tissues than in normal skin samples by qRT-PCR analysis.

Enzymes GLUT1 and HK2 catalyze the first step of glycolysis, while 6-phosphofructo-2-kinase/fructose-2,6-biphosphatase 3 (PFKFB3) is involved in one of the rate-limiting steps of glycolysis.[21] Fibroblasts separated from keloid tissue expressed higher levels of HK2 and PFKFB3 than normal skin fibroblasts, while hypertrophic, proliferative stage, and atrophic scars did not express these proteins.[8] An intracellular metabolic profile assay by western blotting indicated that fibroblasts underwent reprogramming of their metabolic phenotype from OXPHOS to anaerobic glycolysis (Warburg effect).[8] Fibroblasts localized in the CZ of nodules expressed autophagic markers (LC3, p62) and high levels of glycolytic enzymes. Furthermore, cancer cells use recycled and high-energy nutrients (ketone bodies, L-lactate, glutamine, etc) produced by autophagy. The reverse Warburg effect suggests the possibility that stromal-epithelial metabolic coupling, involving high-energy nutrient transfers, occurs between cancer cells and cancer-associated fibroblasts.[22,23] In the first step of the reverse Warburg effect, the cancer cells induce oxidative stress and autophagy to stromal fibroblasts. Then, the tumor stroma exports lactate to the cancer cells via MCT4 (the transporter for lactate efflux). In the second step, the cancer cells import lactate via MCT1 (the transporter for lactate influx).[24] Studies on human breast cancer have found that MCT4 and HIF1α-positive cancer-associated fibroblasts and MCT1 and HIF2α-positive cancer cells make a unit-like structure, and cancer nests are surrounded by cancer-associated fibroblasts.[25,26] In our previous study on keloid nodules, we found the same structure as the above studies, including selective upregulation of MCT4 and HIF1α in CZ fibroblasts and significant upregulation of HIF2α in MZ fibroblasts.[2] Our TEM study showed that CZ fibroblasts containing autophagic vacuoles and MZ fibroblasts showing active features like myofibroblasts showed the progressive development of rER.[27,28] These results suggested that CZ and MZ fibroblasts play different roles in the Warburg effect.

Pyruvate kinase M1 expression is abundant in high-energy demanding organs (eg, the brain and muscles), and PKM2 is expressed in various proliferating cells (eg, embryonic and tumor cells).[16] Several studies reported that the upregulation of PKM2 induces reprogramming of the Warburg effect in cancer cells. It has been proposed that the PKM isoforms switch from PKM1 to PKM2 to establish the Warburg effect during carcinogenesis and that PTBP1 is expressed in PKM2-dominant tissues.[17] The mRNA gene and protein expression levels of PKM2 were significantly higher in keloid fibroblasts than in normal skin fibroblasts; the expression levels in other types of scar fibroblasts were, however, lower than in normal skin fibroblasts.[8,29] Our western blotting analysis demonstrated that a higher expression of PKM2 in keloids supported a higher expression of glycolytic enzymes in keloid fibroblasts, which suggests that PKM2 induces the reprogramming of the Warburg effect in keloid fibroblasts. In

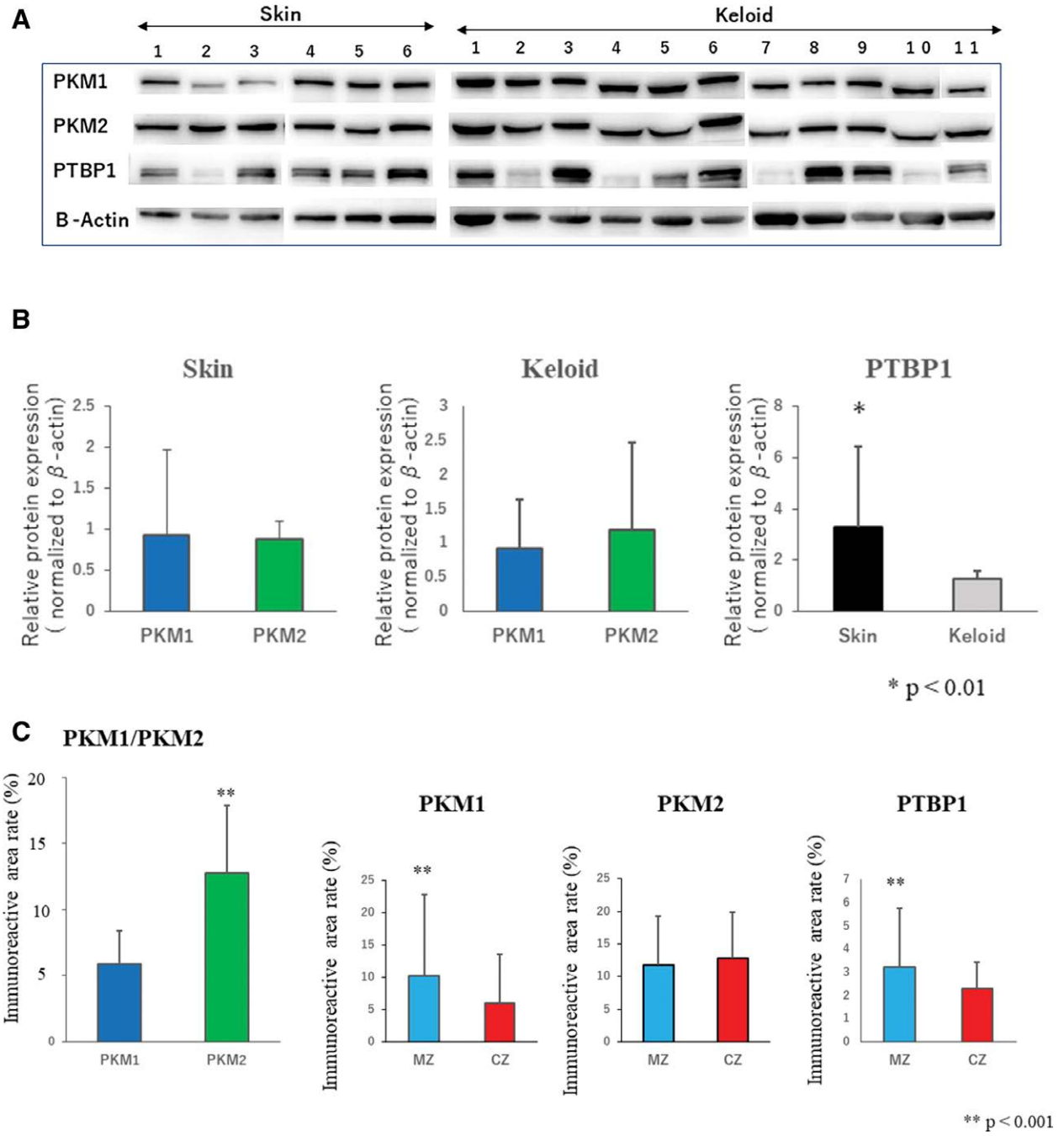

Fig. 3. The Warburg effect occurred in the keloid nodule. A, Western blotting analysis of the Warburg effect proteins (PKM1, PKM2, PTBP1) in the skin and keloid tissue. B, Normalized blotting bands by β-actin. Equal expression of PKM1 and PKM2 in skin (n.s.) and high expression of PKM2 in keloid tissue. Remarkably high expression of PTBP1 in skin ($P < 0.01$) and low expression in keloid tissue. Numbers represent the relative expression ratio (miRNA/RNU6B) with the skin taken as 1.0. C, ImageJ analysis of the Warburg effect markers for nodules. Total PKM2 expression in whole nodules was significantly higher than that of PKM1 (**$P < 0.001$). PKM1 and PTBP1 levels were higher in the MZ than in the CZ (**$P < 0.001$), whereas the opposite was true for PKM2 expression. Numbers represent the percentage of the immunoreactive area per zone.

contrast, the higher expression of PTBP1 in normal skin compared with keloids may be due to the high expression of PTBP1 in all epidermis layers (except that of the cornea), which consist of proliferating basal and differentiating granular keratinocytes (Human Protein Atlas; **https://www.proteinatlas.org**). In a previous study, a xenograft model, where human breast cancer cells (MDA-MB-231) and fibroblasts overexpressing PKM1 or PKM2 were co-injected into nude mice, showed an increase in the growth of co-injected MDA-MB-231 cells. The IHC analysis of

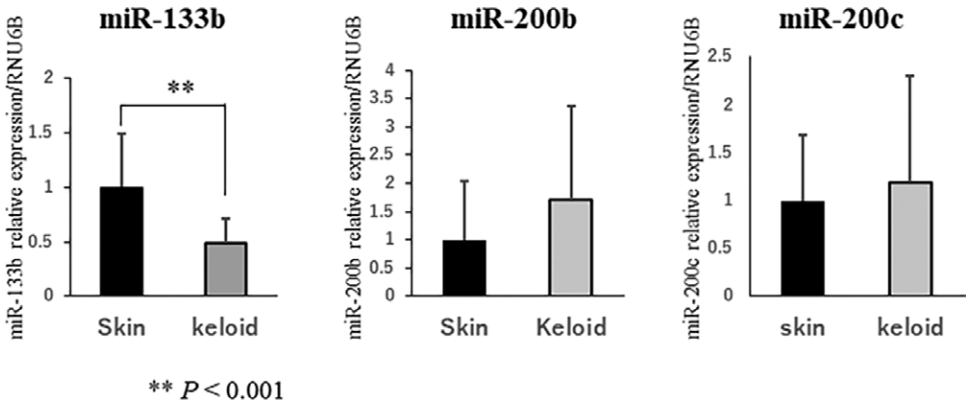

Fig. 4. MiR-133b is a key regulator for PTBP1 in keloids. The qRT-PCR tests were used to analyze the expression of miR-133b, miR-200b, and miR-200c in the skin and keloid tissue; statistically significant lower miR-133b expression was observed in keloid tissue (**$P < 0.001$).

the cancer samples revealed that PKM1 and PKM2 were highly expressed in the cancer stroma.[30] Western blot tests indicated that PKM2 expression was higher in keloids than in the normal skin; in addition to this expression, IIHC analysis revealed characteristic localization of PKM and PTBP1. In the nodules, the total PKM2-positive area was significantly greater than the total PKM1-positive area. The extent of PKM2-positive areas were moderately higher in the CZ and slightly higher than in the MZ than the respective areas in PKM1. Furthermore, in the CZ, the distribution of PKM2-positive fibroblasts was higher than of PKM1-positive fibroblasts. In contrast, the PKM1- and PTBP1-positive areas were highly expressed in the MZ than the CZ. These results raise questions on the mechanisms by which PKM1-positive fibroblasts in the CZ are converted to PKM2-positive fibroblasts because of the low expression of PTBP1.

MiR-133b, a miRNA targeting PTBP1, is expressed in a tissue-specific manner in muscle tissue, colorectal cancer, gastric cancer, and rhabdomyosarcoma.[16,17] In this study, an extensive analysis of the Target Scan Human 7.2 website identified 26 candidate miRNAs (including miR-133b, miR-200b, c) for *PTBP1*. MiRNA expression profiles using miRNA microarrays showed that 264 miRNAs were significantly differentially expressed by greater than twofold between keloid tissue and normal skin. Of those, nineteen miRNAs, including miR-133a, b, and miR-200b and c, were the most downregulated.[18,31] MiRNAs have multiple targets and functions. According to the TargetScan website, miR-133b is the potent regulator of α1(I) and/or α2(II) collagen. In skin fibrosis, miR-133b is downregulated in the scleroderma and keloid.[32] In this study, miR-133b was downregulated in keloid tissue, meaning that miR-133b may promote the expression of *PTBP1* and some fibrosis-related genes. Thus, this short RNA may potentially be a target for oligonucleotide therapeutics, which inhibit the Warburg effect in keloid nodules.

Our study findings support the notion that the Warburg effect occurs in keloid nodules, more specifically in the CZ area of the nodules. The TEM results showing the distinct characteristic features of fibroblasts in both zones suggested that the MZ and CZ play different roles during the Warburg effect. Furthermore, the significantly high numbers of PKM2-positive areas indicated that the Warburg effect occurs in the nodules. With several PTBP1- and PKM1-positive areas being localized in the MZ, the PKM2-positive area was smaller in the MZ than in the CZ, which had a small PTBP1-positive area. We further confirmed the downregulation of miR-133b targeting *PTBP1* in keloid tissue. However, we did not verify that PTBP1 was activated after the downregulation of miR-133b in MZ fibroblasts. Based on these results, we propose distinct roles for the two nodule zones in the Warburg effect. We hypothesize that the CZ could be the center for glycolysis, supplying lactate to the MZ. It is at the MZ that PTBP1 would be activated by the downregulation of miR-133b and PKM1-positive fibroblasts would be converted into PKM2-positive fibroblasts, which are then presented to the CZ (Fig. 5).

It is important to note that in this study there were some limitations. First, we used nonadjacent normal skin tissues as controls for western blot and qRT-PCR analyses. Second, the disease duration, which is important for nodule formation,[3] was inconsistent in our samples. Third, we verified the Warburg effect using IHC analysis and qRT-PCR tests on keloid tissue. However, there was a lack of effective keloid animal models, and purified cultured fibroblasts from keloid samples for in vitro experiments do not share the same status as fibroblasts in keloid tissue or nodules.[33] Thus, further studies to verify the effects of miR-133b-3p for keloid fibroblasts (eg, miRNA transfer experiment in vitro and ex vivo) are needed to better understand these mechanisms.[17,20,34]

CONCLUSIONS

Here, we showed that the Warburg effect occurred in each nodule of the keloids, with the two zones of the keloid playing different roles in the Warburg effect.

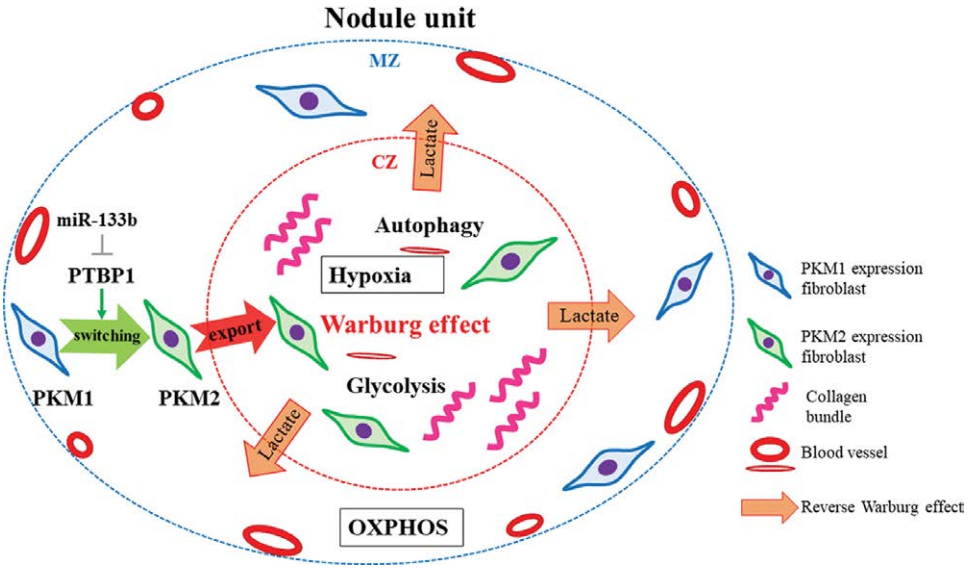

Fig. 5. The role of the CZ and MZ in the Warburg effect. In the hypoxic CZ, increased glycolysis (Warburg effect in CZ fibroblasts) and enhanced autophagy occurred to remove oxidative stress and generate energy (including lactate) for MZ fibroblasts (reverse Warburg effect). Downregulation of miR-133b-3p occurred in keloid nodules. The higher expression of PTBP1 in normoxic OXPHOS-MZ may promote PKM1-positive fibroblasts to PKM2-positive fibroblasts, which may be exported to CZ, accelerating the execution of the Warburg effect in the CZ.

MiR-133b was predicted to control the Warburg effect by activating PTBP1 in keloids, and is a potential candidate for oligonucleotide therapeutics for keloid treatment.

Yuko Ito, MD, PhD
Department of General and Gastroenterological Surgery
Osaka Medical and Pharmaceutical University
2-7 Daigaku-machi, Takatsuki
Osaka 569-8686
Japan
E-mail: yuko.ito@ompu.ac.jp

DISCLOSURE

The authors have no financial interest to declare in relation to the content of this article.

ACKNOWLEDGMENTS

We would like to thank Akiko Miyamoto at the Laboratory of General and Gastroenterological Surgery, as well as Rintaro Oide and Akiko Kagotani at the Translational Research Program, Osaka Medical and Pharmaceutical University, for their strong technical support.

REFERENCES

1. Ueda K, Furuya E, Yasuda Y, et al. Keloids have continuous high metabolic activity. *Plast Reconstr Surg.* 1999;104:694–698.
2. Okuno R, Ito Y, Eid N, et al. Upregulation of autophagy and glycolysis markers in keloid hypoxic-zone fibroblasts: morphological characteristics and implications. *Histol Histopathol.* 2018;33:1075–1087.
3. Ueda K, Lee Y, Inomata Y, et al. Keloid nodule metabolic activity for continuous expansion. *Plast Reconstr Surg Glob Open.* 2022;10:e4492.
4. Warburg O. On the origin of cancer cells. *Science.* 1956;123:309–314.
5. Liberti MV, Locasale JW. The Warburg effect: how does it benefit cancer cells? *Trends Biochem Sci.* 2016;41:211–218.
6. Pavlides S, Whitaker-Menezes D, Castello-Cros R, et al. The reverse Warburg effect: aerobic glycolysis in cancer associated fibroblasts and the tumor stroma. *Cell Cycle.* 2009;8:3984–4001.
7. Vincent AS, Phan TT, Mukhopadhyay A, et al. Human skin keloid fibroblasts display bioenergetics of cancer cells. *J Invest Dermatol.* 2008;128:702–709.
8. Su Z, Jiao H, Fan J, et al. Warburg effect in keloids: a unique feature different from other types of scars. *Burns.* 2022;48:176–183.
9. Taniguchi K, Uchiyama K, Akao Y. PTBP1-targeting microRNAs regulate cancer-specific energy metabolism through the modulation of PKM1/M2 splicing. *Cancer Sci.* 2021;112:41–50.
10. Lu TX, Rothenberg ME. MicroRNA. *J Allergy Clin Immunol.* 2018;141:1202–1207.
11. Rupaimoole R, Slack FJ. MicroRNA therapeutics: towards a new era for the management of cancer and other diseases. *Nat Rev Drug Discov.* 2017;16:203–222.
12. Chakraborty C, Sharma AR, Sharma G, et al. Therapeutic miRNA and siRNA: moving from bench to clinic as next generation medicine. *Mol Ther Nucleic Acids.* 2017;8:132–143.
13. Ratti M, Lampis A, Ghidini M, et al. MicroRNAs (miRNAs) and long non-coding RNAs (lncRNAs) as new tools for cancer therapy: first steps from bench to bedside. *Target Oncol.* 2020;15:261–278.
14. Chakraborty C, Sharma AR, Sharma G, et al. Therapeutic advances of miRNAs: a preclinical and clinical update. *J Adv Res.* 2021;28:127–138.
15. Tran PX, Inoue J, Harada H, et al. Potential for reversing miR-634-mediated cytoprotective processes to improve efficacy of chemotherapy against oral squamous cell carcinoma. *Mol Ther Oncolytics.* 2022;24:897–908.
16. Taniguchi K, Sugito N, Shinohara H, et al. Organ-specific microRNAs (MIR122, 137, and 206) contribute to tissue characteristics

and carcinogenesis by regulating pyruvate kinase M1/2 (PKM) expression. *Int J Mol Sci* . 2018;19:1276.
17. Taniguchi K, Sakai M, Sugito N, et al. PTBP1-associated microRNA-1 and -133b suppress the Warburg effect in colorectal tumors. *Oncotarget*. 2016;7:18940–18952.
18. Zhong L, Bian L, Lyu J, et al. Identification and integrated analysis of microRNA expression profiles in keloid. *J Cosmet Dermatol*. 2018;17:917–924.
19. Eid N, Ito Y, Maemura K, et al. Elevated autophagic sequestration of mitochondria and lipid droplets in steatotic hepatocytes of chronic ethanol-treated rats: an immunohistochemical and electron microscopic study. *J Mol Histol*. 2013;44:311–326.
20. Inomata Y, Oh JW, Taniguchi K, et al. Downregulation of miR-122-5p activates glycolysis via PKM2 in Kupffer cells of rat and mouse models of non-alcoholic steatohepatitis. *Int J Mol Sci* . 2022;23:5230.
21. Yetkin-Arik B, Vogels IMC, Nowak-Sliwinska P, et al. The role of glycolysis and mitochondrial respiration in the formation and functioning of endothelial tip cells during angiogenesis. *Sci Rep*. 2019;9:12608.
22. Pavlides S, Vera I, Gandara R, et al. Warburg meets autophagy: cancer-associated fibroblasts accelerate tumor growth and metastasis via oxidative stress, mitophagy, and aerobic glycolysis. *Antioxid Redox Signal*. 2012;16:1264–1284.
23. Wilde L, Roche M, Domingo-Vidal M, et al. Metabolic coupling and the reverse Warburg effect in cancer: implications for novel biomarker and anticancer agent development. *Semin Oncol*. 2017;44:198–203.
24. Whitaker-Menezes D, Martinez-Outschoorn UE, Lin Z, et al. Evidence for a stromal-epithelial "lactate shuttle" in human tumors: MCT4 is a marker of oxidative stress in cancer-associated fibroblasts. *Cell Cycle*. 2011;10:1772–1783.
25. Witkiewicz AK, Whitaker-Menezes D, Dasgupta A, et al. Using the "reverse warburg effect" to identify high-risk breast cancer patients: stromal MCT4 predicts poor clinical outcomes in triple-negative breast cancers. *Cell Cycle*. 2012;11:1108–1117.
26. Chiavarina B, Martinez-Outschoorn UE, Whitaker-Menezes D, et al. Metabolic reprogramming and two-compartment tumor metabolism: opposing role(s) of HIF1α and HIF2α in tumor-associated fibroblasts and human breast cancer cells. *Cell Cycle*. 2012;11:3280–3289.
27. Bell RE, Shaw TJ. Keloid tissue analysis discredits a role of myofibroblasts in disease pathogenesis. *Wound Repair Regen*. 2021;29:637–641.
28. Hahn JM, McFarland KL, Combs KA, et al. Myofibroblasts are not characteristic features of keloid lesions. *Plast Reconstr Surg Glob Open*. 2022;10:e4680.
29. Li Q, Qin Z, Nie F, et al. Metabolic reprogramming in keloid fibroblasts: aerobic glycolysis and a novel therapeutic strategy. *Biochem Biophys Res Commun*. 2018;496:641–647.
30. Chiavarina B, Whitaker-Menezes D, Martinez-Outschoorn UE, et al. Pyruvate kinase expression (PKM1 and PKM2) in cancer-associated fibroblasts drives stromal nutrient production and tumor growth. *Cancer Biol Ther*. 2011;12:1101–1113.
31. Liu Y, Yang D, Xiao Z, et al. MiRNA expression profiles in keloid tissue and corresponding normal skin tissue. *Aesthet Plast Surg*. 2012;36:193–201.
32. Babalola O, Mamalis A, Lev-Tov H, et al. The role of microRNAs in skin fibrosis. *Arch Dermatol Res*. 2013;305:763–776.
33. Sun H. Metabolic reprogramming and Warburg effect in keloids. *Burns*. 2022;48:1266–1267.
34. Yang W, Tan S, Yang L, et al. Exosomal miR-205-5p enhances angiogenesis and nasopharyngeal carcinoma metastasis by targeting desmocollin-2. *Mol Ther Oncolytics*. 2022;24:612–623.